universität wien

MASTERARBEIT / MASTER'S THESIS

Titel der Masterarbeit / Title of the Master's Thesis

„Duality Between Classical Waves and Particles“

verfasst von / submitted by

Polina Pogrebinskaya, BSc

angestrebter akademischer Grad / in partial fulfilment of the requirements for the degree of

Master of Science (MSc)

Wien, 2021 / Vienna, 2021

Studienkennzahl lt. Studienblatt / degree programme code as it appears on the student record sheet:	UA 066 876
Studienrichtung lt. Studienblatt / degree programme as it appears on the student record sheet:	Masterstudium Physik
Betreut von / Supervisor:	Ass.-Prof. Mag. Dr. Borivoje Dakić

Acknowledgements:

Borivoje Dakić for the guidance, support and knowledge. My colleagues in the ***Operational Quantum Information Group***, in particular ***Fatemeh Bibak*** for her continuous assistance and thorough advice, ***Joshua Morris*** for his patience and help at the early stages of the project.

1 Abstract

Interference of single particles lies at the core of quantum mechanics. The most prominent demonstration of this effect is the double-slit experiment: the presence of a quantum particle is verified by a single spot on the detection screen. While this clearly indicates an experiment with particle-like objects, the statistics of repeated runs reassembles interference fringes. This observation is the source of the wave-particle duality and it is dedicated to genuine quantum behavior. Nonetheless, it is unclear whether this conclusion is justified and to which extend we can reproduce such an experiment with classical waves? In this work we show that standard (classical) wave mechanics combined with the statistical detection model completely reproduces quantum interference experiments with single particles. We dubbed this phenomenon the "classical particle-wave duality". The recreation of an interference pattern of a quantum double-slit experiment using classical waves shows that the "unusual behavior" of quantum systems in this experiment is not necessarily proof of a genuine quantum effect.

Zusammenfassung

Die Interferenz einzelner Teilchen ist der Kern der Quantenmechanik. Die prominenteste Demonstration dieses Effekts ist das Doppelspaltexperiment: Die Anwesenheit eines Quantenteilchens wird durch einen einzelnen Fleck auf dem Detektionsschirm bestätigt. Während dies eindeutig auf ein Experiment mit partikelähnlichen Objekten hinweist, setzt die Statistik wiederholter Durchläufe Interferenzstreifen wieder zusammen. Diese Beobachtung ist die Quelle des Welle-Teilchen-Dualität und ist dem echten Quantenverhalten gewidmet. Es ist jedoch unklar, ob diese Schlussfolgerung berechtigt ist und inwieweit wir ein solches Experiment mit klassischen Wellen reproduzieren können? In dieser Arbeit zeigen wir, dass die (klassische) Standardwellenmechanik in Kombination mit dem statistischen Detektionsmodell Quanteninterferenzexperimente mit einze--lnen Teilchen vollständig reproduziert. Wir haben dieses Phänomen als „klassische Teilchen-Welle-Dualität“ bezeichnet. Die Nachbildung eines Quanten-Doppelspalt-Experiments mit klassischen Wellen zeigt, dass das „ungewöhnliche Verhalten“ von Quantensystemen in diesem Experiment nicht unbedingt ein Beweis für einen echten Quanteneffekt ist.

Contents

1 Abstract **2**

2 Introduction **5**

3 Quantum Wave- Particle Duality **6**
3.1 Double-Slit Interference 7
3.2 Single-particle Interference 9

4 "Classical Wave- Particle Duality" **10**
4.1 Detection Model 10

5 Simulated results **13**
5.1 Interference pattern 13
5.2 Numerical simulation 15

6 Poisson Limit **18**
6.1 Analytical derivation of the Poisson Limit 19
6.2 Post-selection 20

7 Conclusion and Outlook **21**

8 Appendix **22**

2 Introduction

The quantum nature of the interference of single particles was first observed in 1927 through the double slit experiment: a source emits a single quantum particle (photon or electron) per experimental run, which then passes through a screen with two slits. The presence of a particle is then detected by a single spot (detection click) on the observation screen. While this clearly indicates an experiment with particle-like objects, the statistics of repeated experimental runs reassembles interference fringes (characteristic property for waves). The formation of interference by individual particles is the source of the wave-particle duality. The particles are observed as such at the source and on the screen, however, behave as waves, described by the wave function, in between. This effect was notably questioned by Einstein: "the apparent difficulty in this description is that the detection of a particle at point "A" eliminates the detection of the particle at point "B", although the rules of ordinary wave propagation offer no room for such an event" [1].

The aim of the thesis is to investigate the existence of a regime in classical wave mechanics, which can simulate the quantum interference of single particles. More precisely, we are looking for a domain of parameters that recreate a single click per experimental run (particle behavior) in addition to the statistics of clicks displaying an interference pattern (wave behavior). We proceed under the assumption that detection of classical waves is probabilistic, with intensity- dependent probability. It follows that if the incident intensity is zero, there will be no clicks at the detection screen. If, on the other hand, the incident intensity is high the amount of detection events per run is expected to be very high, thus recreating the classical wave interference pattern. Thereby, by slowly varying the incoming intensity we should be able to find a regime that will model the individual experimental runs with a single detection event (one particle), while the statistics of repeated runs will form an interference pattern of the double slit experiment.

In order to demonstrate this result we will generate a numerical simulation of the double slit experiment with: a classical wave source, a 2-dimensional configuration of the slits, the assumption that the experiment is simulated in the far-field region (the detection screen is sufficiently far away from the light source) and the screen is a collection of point-like probabilistic detectors. After simulating the high intensity experiment we will lower the intensity to zero and slowly increase it to enter the single click-per-run detection regime. Our aim is to perform a simulation of a real-time formation of the interference pattern.

On the other hand, the proof of the validity of the result shall be obtained from analytical study of the measurement pattern via the Poisson limit theorem [2], as follows. In the model, we treat the incoming light as a classical electromagnetic wave. The incoming wave is incident at a point on the screen where it probabilistically activates the detector. The probability of detection varies in accordance with a certain threshold directly proportional to the light intensity, i.e. the detector either registers a click or remains silent. We divide our screen into N detectors (where N is large) and proceed with determining the overall detection pattern. Since there are two outcomes for each detector, it is convenient to use a binomial distribution to determine the

resulting distribution of "clicks" and "no-clicks" for N detectors. Lowering the incoming intensity to zero should result in a Poisson distribution. Finally, the parameters of the Possion distribution are tuned such that the probability of a single detection event (per run) significantly dominates all other events. Post-selecting only the experimental runs in which there was an event detected, in other words, discarding all of the "vacuum" runs, enables us to achieve a regime in which only a single event is detected per run or no events at all.

This approach enables us to completely reassemble interference of single quantum particles by using classical waves. The recreation of the results of the double-slit experiment using classical waves shows that the "unusual behaviour" of the single-photons/electrons is not necessarily proof of a genuine quantum effect.

In this work we begin with a short overview of the quantum wave-particle duality, in section 3. We then proceed to describe the theoretical concepts behind its classical realisation, in section 4. Section 5 is dedicated to the numerically simulated results. Finally, in section 6 we explore the analytical derivation of the Poisson limit, followed by the derivation of the exact single-click per experimental run regime via post-selection. This work is concluded with some closing remarks, analysing the limitations of the work, as well as a potential outlook.

3 Quantum Wave- Particle Duality

Prior to the discovery of light quantization by Albert Einstein, light was largely regarded as a wave. The wave- like nature of light was reflected in experiments by Fresnel and Young, where an interference pattern was observed after an incident light ray would pass through a grating. The interference pattern is indicative of constructive and destructive wave interference, where the wave intensity is increased or nullified, respectively. Forming a pattern of light and dark fringes. James Clerk Maxwell was further able to investigate the nature of the light wave by modelling it theoretically [3]. The solutions of the Maxwell equations determined that the electric and magnetic fields travel through space with speed of light. Thereby, finally concluding that light is an electromagnetic wave. Nonetheless, the theory was not sufficient to account for other phenomena associated with light, such as the photoelectric effect.

In the early 20th century Albert Einstein established that light waves with the same frequency were quantized into single quanta, known as a photons [4]. This description interprets photons as "grains" of light with frequency- dependent energy $E = h\nu$, thus explaining the behavior of the electron emission observed in the photoelectric effect. This discovery further complicated the understanding of light as the experimental demonstration of interference is a clear indication of its wave-like nature, whereas the quantization of light is evidence of particle-like behaviour [5]. An interpretation of the phenomena was again proposed by Albert Einstein. According to Einstein's solutions of the equations for thermodynamic fluctuations, light was both a wave and a particle. The equation presented a term known as "shot noise" to account for a "random particle" and a term known as "speckle" to account for a "random wave" [4]. The

theory was further extended by Luis de Broigle to state that, the duality of wave- and particle-like characteristics was not specific to only light. Rather that particles, such as electrons, too could be described as a wave. An experimental validation of this statement was demonstrated by the double-slit experiment [6].

3.1 Double-Slit Interference

"The double slit experiment is absolutely impossible to explain in any classical way and has in it the heart of quantum mechanics. In reality, it contains the only mystery" [7] - R.P. Feynman

First introduced by C. Davisson and L. Germer in 1927 [6], the set-up consists of a source, a double-slit grating and a detection screen, placed a sufficient distance away. Initially, the source emits light continuously with an intensity that is sufficiently high, so that the incident light is regarded as a wave. As seen on figure 1, an interference pattern can be observed on the detection screen. The pattern can be explained with classical wave mechanics: the outgoing waves interfere, forming fringes [8].

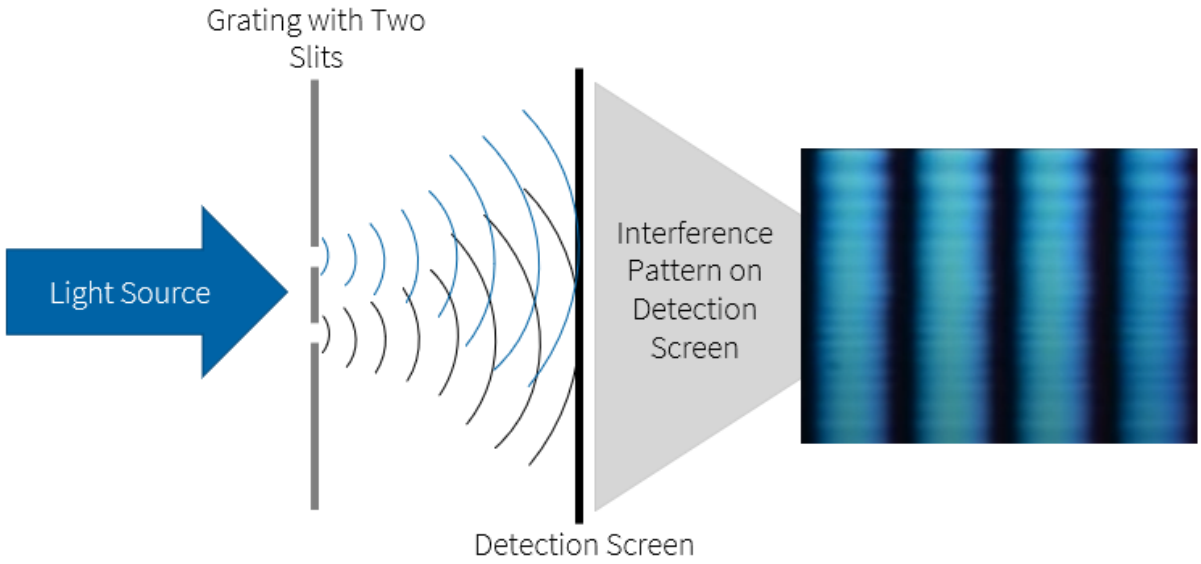

Figure 1: The double-slit experiment set-up with a wave source.

The light source is then attenuated so as ensure that approximately one single photon is emitted per an experimental run. Sensibly, a single event is observed on the detection screen, demonstrating a presence of a particle.

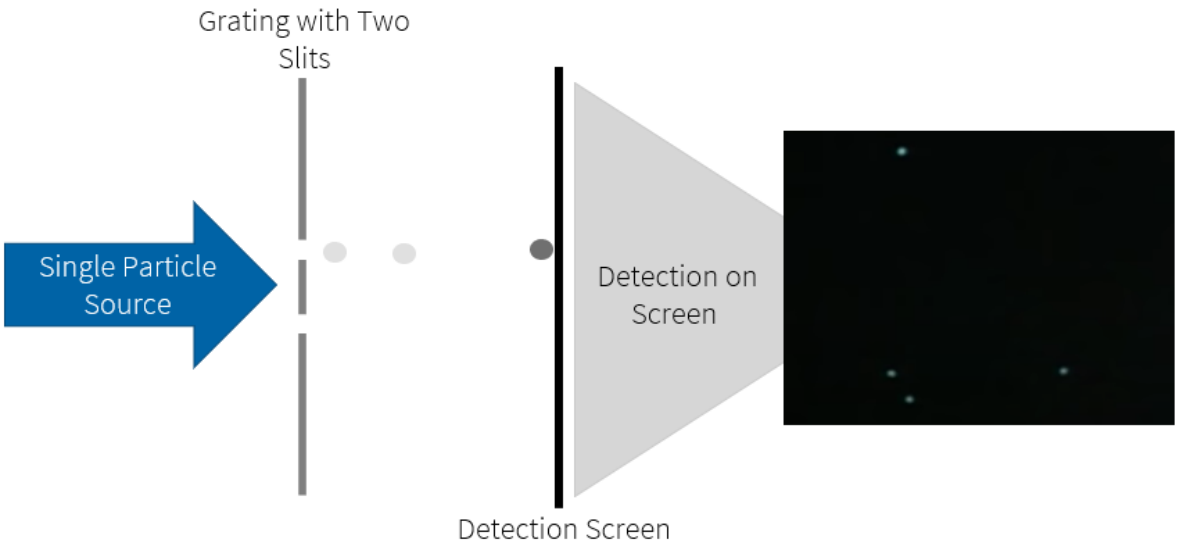

Figure 2: The double-slit experiment set-up with a "single particle" or attenuated light source after one experimental run.

The experiment is repeated and as the amount of runs increases a pattern emerges on the detection screen [8]. As the number of runs becomes very large the observed pattern resembles that of the interference of light waves.

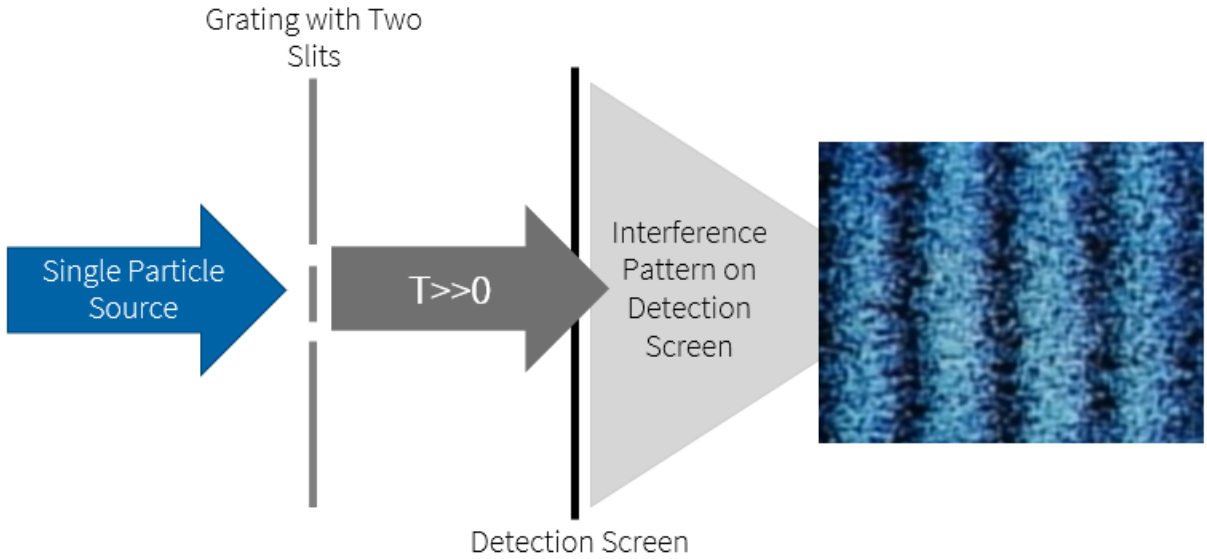

Figure 3: The double-slit experiment set-up with a "single particle" or attenuated light source after many experimental runs.

The idea behind this description is that the particle-like objects behave as such at the source and the detection screen, however can be described as waves otherwise [9]. This phenomenon

and the build up of the interference pattern is illustrated in Fig. 2 and 3.

3.2 Single-particle Interference

The theoretical description of light as a single quanta of energy, the photon, proceeds its experimental verification: there were no experimental set-ups that could successfully reproduce a single-photon source [10]. Further investigation was inspired by the idea that, instead of looking at single detection events one must look at coincidence rates. A set-up was proposed by A. Aspect and P. Grangier in 1985, see figure 4 [11]. If a wave is incident on a beam splitter a part of it will be reflected, while the other is transmitted. If a detector is placed along each path a click should be registered at each detector, as neither the reflection, nor the transmission probabilities are zero for a classical wave [12]. It is then possible to place a detector to register the coincidence rates for the transmitted and reflected wave paths. The third detector- coincidence detector, can be linked to the other two and if the detectors register a click at the same time, the third detector will register a coincidence count.

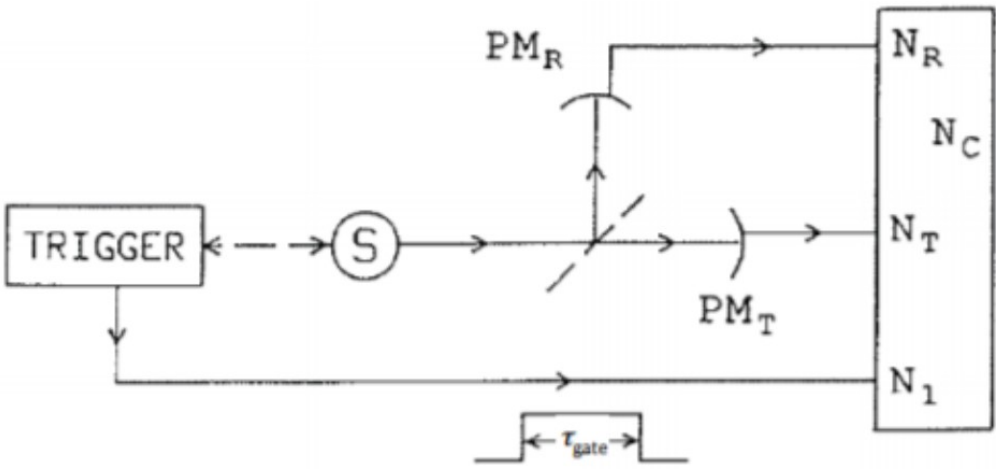

Figure 4: The source S emits light pulses, the beam splitter splits the pulse into the transmitted and reflected components. N_R and N_T are the rates of single detection, N_C is the coincidence rate [11]

If, however, the experiment is repeated with a single particle (photon or electron) source, the beam splitter wouldn't be able to split the particle into two parts. Meaning, there is only one path that the particle will take and only one of the two detectors will click per one experimental run. Hence, the probability of registering a coincidence by the third detector in this scenario has to be equal to zero. Nonetheless, registering a zero coincidence rate experimentally proved to be a bigger challenge, due to background noise detection. Thus a new parameter was introduced to describe the nature of the input light through the detected coincidence rates.

$$\alpha = \frac{P_C}{P_1 P_2} \tag{1}$$

Here, P_C is the probability of coincidence detection, P_1 and P_2 are the probabilities of observing a detection event in detectors one or two. As mentioned before, in order for the source to be an ideal single-particle source $P_C \stackrel{!}{=} 0$, which would result in $\alpha = 0$ and in the realistic experimental case P_C would yield a very small value, making $\alpha < 1$. In other words, an $\alpha < 1$ indicates an experiment with single particles- a single-photon light source and $\alpha \geq 1$ indicates an experiment with a wave-like light source [13][10].

The first successful experiments with a set-up similar to that described above were done in 1985, simultaneously, by A. Aspect, P. Grangier and G. Roger in Orsay and L. Mandel and Chung Ki Hong in Rochester [10]. Prior to these experiments, it was generally believed that the attenuation of a light source was enough to observe particle interference of the double-slit experiment. Nonetheless, when a strongly attenuated light source was used in the 1985 experiment by A. Aspect and P. Grangier it was observed that the probability of coincidence detection was not negligible. In fact the resulting parameter $\alpha = 1.07 \pm 0.08$ [11], violating the single photon bound. Based on this observation, a new description of strongly attenuated light was established known as *coherent light* [11]: faint light which is regarded as quasi-classical with $\alpha \simeq 1$. Coherent light cannot be regarded as a single-photon source as it does not have a well defined photon number. When the experiment is repeated with a coherent light source the light intensity is tuned so as to ensure that on average no photons will be incident on the beam splitter with the probability of $\approx 99\%$. In this case the probability of a single photon being incident on the beam splitter is $\approx 1\%$. However, the Poissonian statistics that describe the characteristics of coherent light, allow for a very small possibility of two-photon production in a single experimental run, thereby resulting in larger coincidence count [10].

4 "Classical Wave- Particle Duality"

4.1 Detection Model

Within classical wave mechanics, one may try naively to describes the possibility of replicating the interference of single particles (observed in figure 3) using the statistical properties of classical electro-magnetic waves [14]. In such models, these statistical properties are attributed to the fluctuation of the incident wave intensities. In this work, we take the opposite route: the incident wave does not have any fluctuations, they will all arise due to the statistical modeling of the detection process. One can see our model as an approach where the incident light is classical while its detection is describes via quantized matter (atoms) [15]. Hence, I introduce a system in which a classical electro-magnetic wave in emitted from the source and incident on the double-slit grating. It is of significance to define the assumption upon which this model is based: the set-up is that of a standard double-slit experiment however the detection screen is modelled by an $N \times M$-dimensional grid, as seen on figure 5. The propagating light wave has a certain probability (proportional to the intensity) of being detected at any point of the grid. This system can be described using a statistical model of stochastic variables. The detection of an event at any location on the detection grid is not deterministic. On the contrary- if the incoming intensity

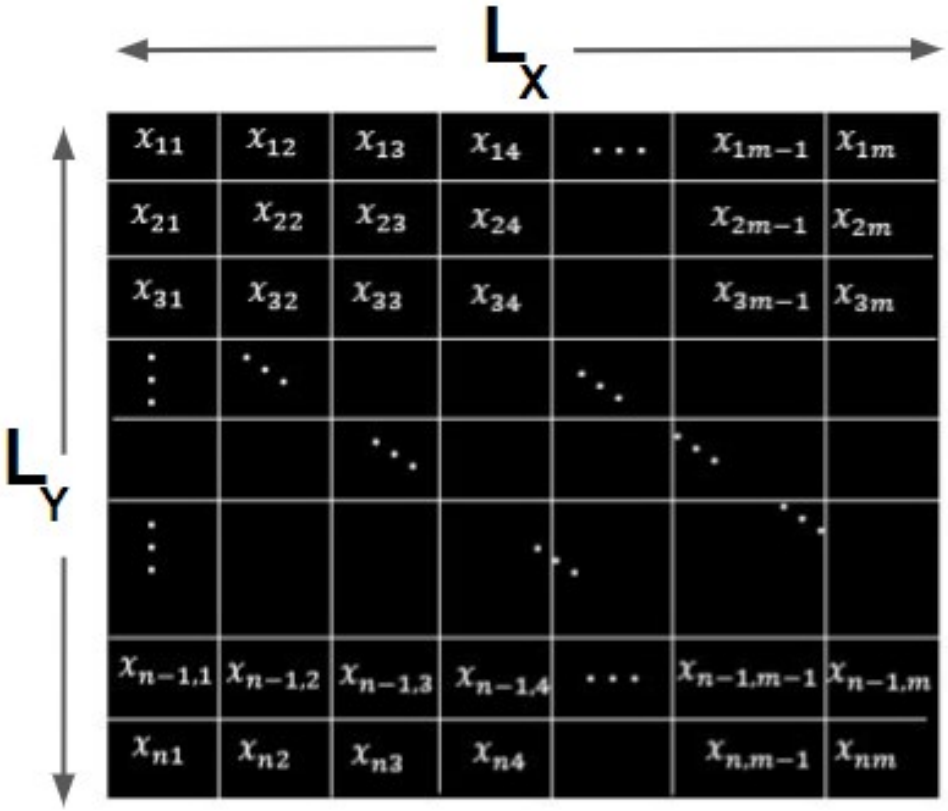

Figure 5: The detection screen divided into an MxN-detection grid. Each point at the detection grid is denoted by x_{mn}

is large, then the probability of detecting an event on the detection grid should be very high- so that the detection pattern, observed on the detection grid, corresponds to the interference pattern of light waves, observed in figure 1. If the intensity of the source is zero, then there will be no detection events observed on the screen [14].

Thereby, if the detection of events is dependent on the incoming wave intensity, then one should be able to find an intensity regime for which one is able to detect a single event on the detection grid. In other words, such a regime will provide a simulation of the detection of a single event per an experimental run. On the other hand, statistics of repeated runs will recreate the particle-wave duality of the single quantum particle interference, observed in the quantum double-slit experiment.

I introduce the detection probability for a single detection unit, located at x_{ij}, to be dependent on the position-dependent outgoing intensity (intensity after passing through the double-slit grating) $I(x)$ and the detection efficiency of the apparatus μ. A single spacing on the

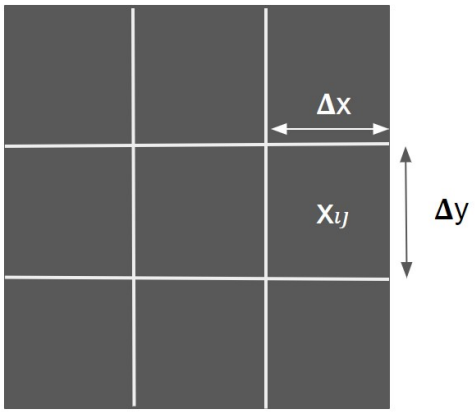

Figure 6: Analytical description of a single detection unit on the detection grid.

grid along the horizontal axis can be expressed as:

$$\Delta x = \frac{L_x}{N}$$

whereby L_x is the width of the grid and N is the total number of the detection units. And a single spacing on the grid along the vertical axis can be expressed as:

$$\Delta y = \frac{L_y}{M}$$

whereby L_y is the height of the grid and M is the total number of the detection units. Hence the area of the detector is then given by:

$$A = L_x \times L_y \tag{2}$$

and the area of a single detection unit is:

$$\delta A = \Delta x \Delta y = \frac{L_x L_y}{N \cdot M} = \frac{A}{N \cdot M}.$$

So the probability of detecting a single click is:

$$p_1(x_{ij}) = \frac{A\mu I(x_{ij})}{N \cdot M} = \mu I(x_{ij}) \delta A \tag{3}$$

Where μ- proportionality constant, here $A\mu$ represents the efficiency of detection per unit area of the detector. Thereby, the corresponding probability of no events being detected at a single detection unit is given by:

$$p_0(x_{ij}) = 1 - p_1(x_{ij}). \tag{4}$$

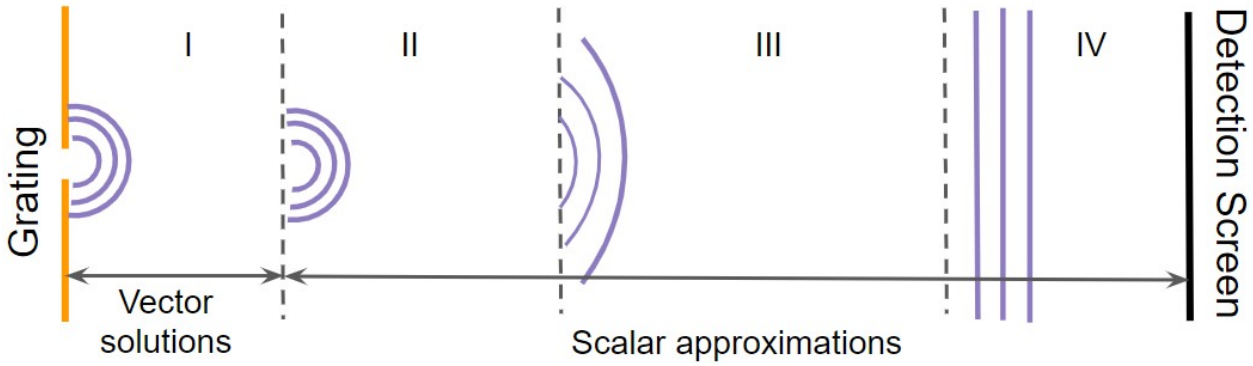

Figure 7: Approximation of the propagation of wave fronts for different diffraction regions. I- full wave equation; II- Rayleigh-Sommerfeld and Fresnel-Kirchoff; III- Fresnel (near-field); IV- Fraunhofer (far-field). [16]

5 Simulated results

In order to perform numerical simulation by using the the detection model from the previous chapter, firstly we shall calculate the intensity patter in the Fraunhofer *far-field* approximation [17] (see Figure 7).

5.1 Interference pattern

Here, we define a set of parameters (depicted in figure 8, left): a denotes the slit width, b is the slit height, d is the distance to the detection screen and L denotes the distance between the slits. The geometry of the setup is shown in Figure 9. The intensity pattern at some location $\vec{r}$ on the detection screen is given by [18]

$$I(\vec{r},t) = |\vec{E}(\vec{r},t)|^2 = |\vec{E}_I(\vec{r},t) + \vec{E}_{II}(\vec{r},t)|^2, \tag{5}$$

with $\vec{E}_{I/II}$ being the contributions of individual slits. We can evaluate these fields by using the Hygens principle and considering each point of the slit (which we call wavelets) as a source of a spherical wave [16]

$$E_W(\vec{r},t) = \frac{e^{i\omega t - ik|\vec{r}-\vec{r}_s|}}{|\vec{r}-\vec{r}_s|}\vec{A}, \tag{6}$$

where $\vec{A}$ is the field amplitude of the wavelet at the location $\vec{r}_s$ and $k = \omega c$.

We shall assume coherent sources for both slits, meaning that this amplitude is simply a constant, independent of the location of the wavelet. The total field is found by integrating over the region of both of the slits:

$$\vec{E}(\vec{r},t) = \vec{A}e^{i\omega t}\int_{\frac{-a}{2}}^{\frac{a}{2}} dx_s \int_0^b dy_s \left(\frac{e^{ik|\vec{r}-\vec{r}_s|}}{|\vec{r}-\vec{r}_s|} + \frac{e^{ik|\vec{r}-\vec{r}_s+\vec{L}|}}{|\vec{r}-\vec{r}_s+\vec{L}|}\right), \tag{7}$$

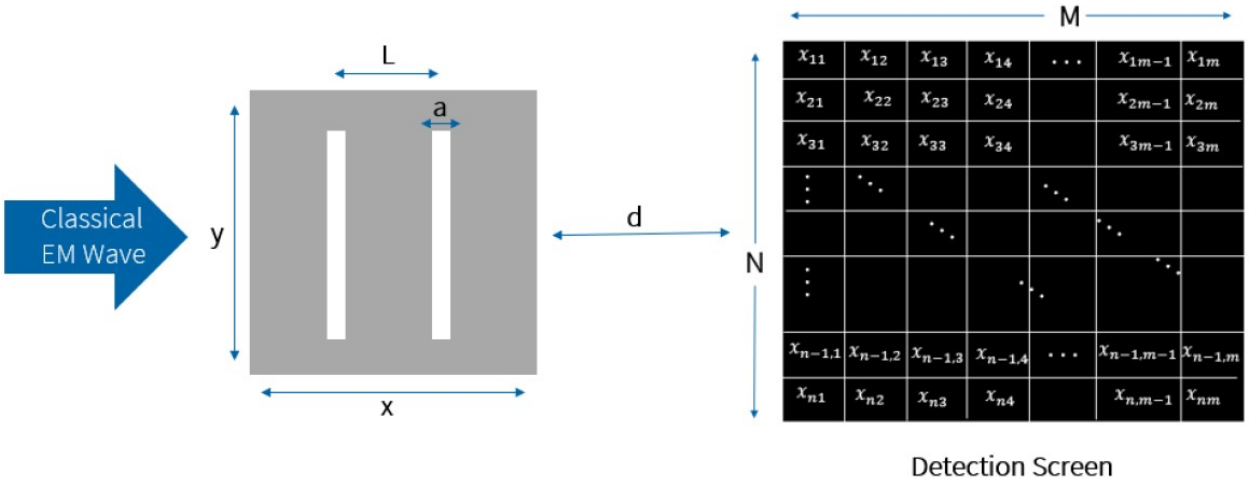

Figure 8: The experimental set-up of the theoretical detection model from section 4. Here L- distance between two slits on the grating, a- width of a single slit, d- distance of grating from the detection grid.

where, $\vec{r}_s = (x_s, y_s, 0)^T$ is the position of the wavelet. For simplicity we introduced $\vec{L} = (L, 0, 0)^T$ to describe the shift of the location of the second slit with respect to the first slit position along the x-axis. Since we are applying the far field approximation, then $d \gg a, L$ we can approximate this integral (via the mean value theorem [1]) to:

$$\vec{E}(\vec{r}, t) \approx \vec{A} e^{i\omega t} ab \left(\frac{e^{ik|\vec{r}-\vec{r}_I|}}{|\vec{r}-\vec{r}_I|} + \frac{e^{ik|\vec{r}-\vec{r}_I+\vec{L}|}}{|\vec{r}-\vec{r}_I+\vec{L}|} \right), \tag{8}$$

where we took $\vec{r}_I = (0, b/2, 0)^T$ to be the location of the slit center and $\vec{r} = (x, y, d)^T$ is the location on the detection screen. Finally, we shall make another set of approximations, i.e.

$$|\vec{r}-\vec{r}_I| = \sqrt{x^2 + (y - \frac{b}{2})^2 + d^2} \approx d \left(1 + \frac{1}{2d^2}(x^2 + (y - b/2)^2) \right). \tag{9}$$

and

$$|\vec{r}-\vec{r}_I+\vec{L}| = \sqrt{(x-L)^2 + (y - \frac{b}{2})^2 + d^2} \approx d \left(1 + \frac{1}{2d^2}((x-L)^2 + (y - b/2)^2) \right). \tag{10}$$

Applying the above approximations enables us to significantly simplify the total intensity formula to the (time and y-direction independent) expression

$$I(\vec{x}) = I_0 \cos^2(\kappa x - \phi), \tag{11}$$

[1] The mean value theorem states $\int_a^b dx f(x) = (b-a) f(x_0)$ for some $x_0 \in [a, b]$ [19]

where we set

$$I_0 = \frac{4ab|\vec{A}|^2}{d^2} \tag{12}$$

$$\kappa = \frac{kL}{2d} \tag{13}$$

$$\phi = \frac{kL^2}{4d}. \tag{14}$$

As we see from the formula above, the intensity patter is time independent and transitional invariant along y-direction, thus the pattern consists of vertical strips which we will confirm in the numerical simulation.

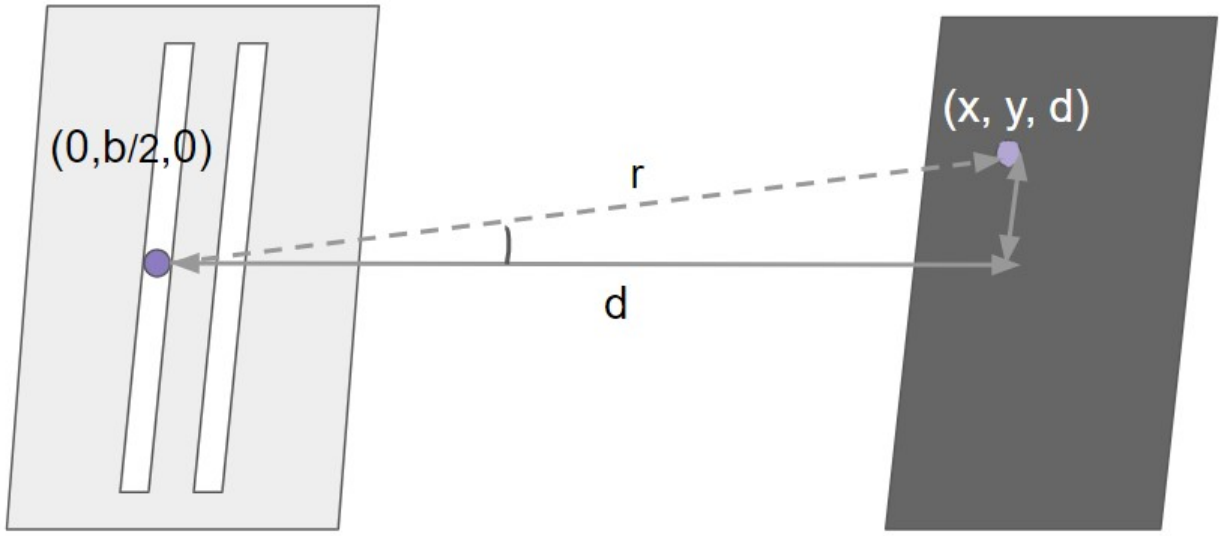

Figure 9: The position of the wavelet as it passes through the grating is indicated by the darker spot on left with coordinates $\vec{r_1} = (0,\ \frac{b}{2},\ 0)$. The position at which an event is registered is indicated by the lighter spot on the right with coordinates $\vec{r} = (x,\ y,\ d)$. The dotted line indicated the position vector r for the detected event.

5.2 Numerical simulation

Following the derivations (for the light intensity) of the last section, I was able to quantify the probability of registering an event (given in equation (3)) for a single experimental run. The simulation of the experiment then proceeds using the following model: the detection probability $p_1(x_{ij})$ given in (3) is applied to generate a $N \times M$ matrix of randomly assigned $0's$ or "$1's$". The parameters for the intensity $I(x)$ formula (11) provided in the last section are fine-tuned such that, for most of the runs, we can observe one detection event per time step. The simulation is repeated for T time steps (runs) and this results in a real time animation of a single click-per-experimental run.

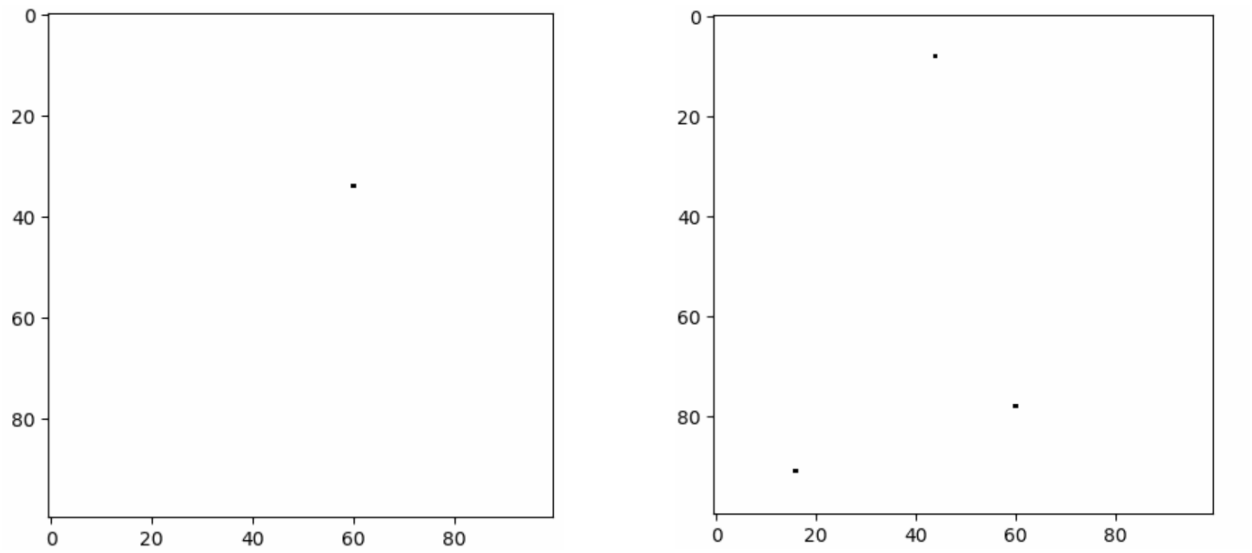

(a) T=1 (b) T=3

Figure 10: The N×M dimensional observation screen after: a)- a single experimental run; b)- three experimental runs. The single dot indicating a single detected event.

The snapshots were taken from the simulated animation for the following conditions: the parameter $k = 2\pi 10^9 m$ (the corresponding wave-length is $\lambda \simeq 10^{-9}$m); the dimensions of the detection grid $M \times N = 1000 \times 1000$, the corresponding initial intensity $I_0 = \frac{1}{10^6} W/m^2$; the phase $\phi = 0$, the distance between the double slit grating and the screen is $d = 2m$, the distance between the distance between the slits $L = 10^{-6} m$, the slit width $a = 10^{-9} m$ and the detection efficiency of each unit on the screen is $\mu = 0.6$. The results are presented in figures 10-12. We clearly on how the interference pattern in built over the time from individual random detection events.

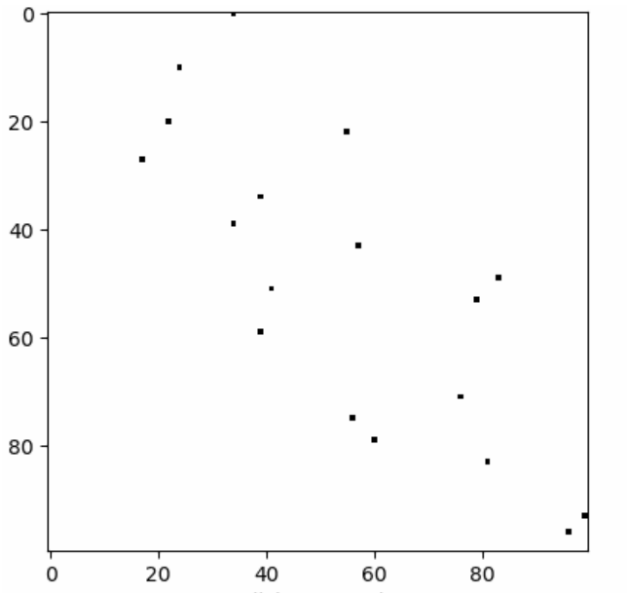

(a) T=10

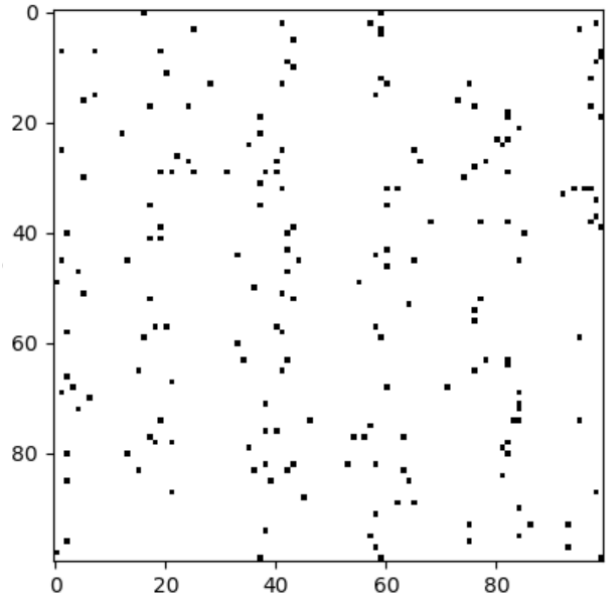

(b) T=100

Figure 11: The N×M dimensional observation screen after: a)- 10 runs; b)- 100 experimental runs, an interference pattern is starting to form.

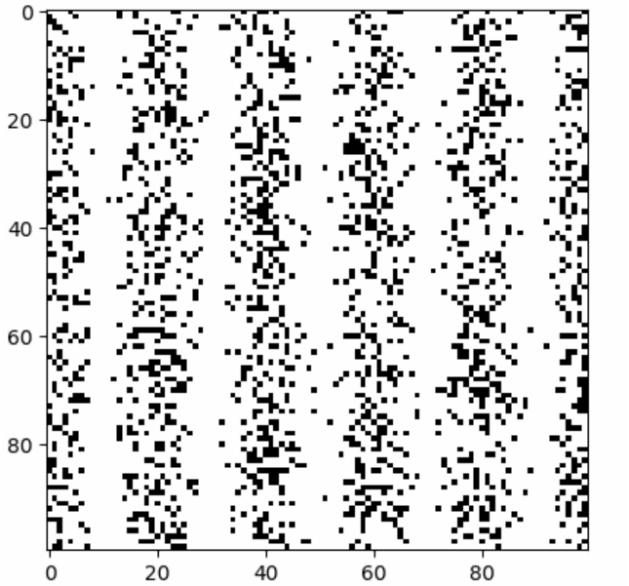

Figure 12: The interference pattern formed by an attenuated classical wave after 1000 experimental runs, reconstructing single particle interference.

6 Poisson Limit

The detection of events at any position on the grid is described by a binomial distribution as every detector can only have one of the two outcomes: "click" or "no click". Furthermore the registration of an event at a single detection unit is completely independent of the registration of an event by any other detection unit of the grid. Hence each detection event is independent of the other and the whole detection process can be viewed as a sum of n independent events, where n is the total number of detection events. I can further speculate: considering that each unit is described by a binomial distribution, as the number of units increases to reach a significantly large amount the detection probability (of detecting n clicks in one repetition) is governed by a Poisson distribution (Poisson limit theorem), as the detection probability scales as 1/[total number of detection units] (see equation (3)). Furthermore, as the detection events are independent but their individual probabilities depend on the location x_{ij} (through the intensity $I(x_{ij})$, one can use a generalized Poission limit theorem- the so-called Le Cam's theorem [20] to approximate the detection probability on the whole grid to be described by the Poisson distribution. Hence, the probability of the detection of n events per unit time shall be given by

$$P_n = e^{-\lambda}\frac{\lambda^n}{n!} \tag{15}$$

In the next section I will prove this formula and consequently derive the corresponding parameter λ (which should depend on the incoming intensity and thereby confirm our numerical simulation given in the previous section).

6.1 Analytical derivation of the Poisson Limit

One can define $R_{ij} = 0, 1$ to be a random variable associated to the outcome of a detection unit $\vec{x}_{ij}$ after each run. Whereby, $R_{ij} = 0$ corresponds to the unit remaining silent "no click" and $R_{ij} = 1$ describes a "click". Thereby, the total number of clicks is then expressed as

$$S = \Sigma_{i=1}^{N} \Sigma_{j=1}^{M} R_{ij} \tag{16}$$

We proceed by deriving a distribution of S in the limit where $N, M \to \infty$. As a starting point, it is reasonable to calculate the characteristic function for S.

$$\chi(t) = \left\langle e^{its} \right\rangle = \Pi_i^N \Pi_j^M e^{itR_{ij}} \tag{17}$$

$$= \Pi_i^N \Pi_j^M (p_1(\vec{x}_{ij}) e^{it \cdot 1}) + (p_0(\vec{x}_{ij}) e^{it \cdot 0}) = \Pi_i^N \Pi_j^M (p_1(\vec{x}_{ij}) e^{it \cdot 1}) + ((1 - p_1(\vec{x}_{ij})) e^{it \cdot 0}) \tag{18}$$

$$= \Pi_i^N \Pi_j^M (p_1(\vec{x}_{ij}) e^{it} + 1 - p_1) = \Pi_{ij} (1 + (e^{it} - 1) p_1(\vec{x}_{ij})). \tag{19}$$

The notation Π_i^N denotes the product over index i running from 1 to N. The following relation holds:

$$\ln \Pi_v a_v = \Sigma_v \ln a_v$$
$$e^{\ln \Pi_v a_v} = e^{\Sigma_v \ln a_v}$$
$$\to \Pi_v a_v = e^{\Sigma_v \ln a_v}$$

so (33) can then be expressed as:

$$\chi(t) = \Pi_{ij} (1 + (e^{it} - 1) p_1(\vec{x}_{ij})) = e^{\Sigma_{ij} \ln (1 + (e^{it} - 1) p_1(\vec{x}_{ij}))} \tag{20}$$

$$= e^{\ln 1} e^{\Sigma_{ij} \ln (e^{it} - 1) p_1(\vec{x}_{ij})} = e^{\Sigma_{ij} \ln (e^{it} - 1) \mu \delta A I(\vec{x}_{ij})} \tag{21}$$

$$\simeq e^{\Sigma_{ij} (e^{it} - 1) \mu \delta A I(\vec{x}_{ij})} = e^{\Sigma_{ij} (e^{it} - 1) \mu \Delta x \Delta y I(\vec{x}_{ij})} = e^{(e^{it} - 1) \mu \int \int_A dx dy I(\vec{x})}, \tag{22}$$

where the integration domain A is the whole detection screen. The characteristic function for the Poisson distribution is given by

$$\chi_{Poisson} = e^{(it-1)\lambda}.$$

Comparing (36) with the characteristic function for the Poisson distribution yields:

$$\lambda = \mu \int \int_A dx dy I(\vec{x}) = \mu \int_0^{L_y} \int_0^{L_x} dx dy I(\vec{x}) \tag{23}$$

Hence, the statistics of the total number of detection events (per experimental run) converges to the Poisson Limit for a very large number of detection units [14]. Furthermore, the expression for the λ parameter allows me to fine-tune the average number of detection events (by changing the intensity parameters). The probability for a single event being detected is given by $P_{n=1} = e^{-\lambda} \lambda$, while the probability for two simultaneous detection events corresponds to $P_{n=2} = e^{-\lambda} \lambda^2 / 2$. The ratio between these two probabilities is given by

$$\frac{P_{n=2}}{P_{n=1}} = \frac{\lambda}{2} = \frac{\mu}{2} \int_0^{L_y} \int_0^{L_x} dx dy I(\vec{x}).$$

As it is clear from this result, the ratio between observing a single event or two events simultaneously (in a single experimental run) is dependent on the incoming intensity. It is reasonable to conclude that a small enough initial intensity should account for minimising the possibility of a simultaneous event detection, however, not excluding that possibility entirely. In the following section we attempt to derive an analytical model for which we can, with determinism, obtain one single click for a single experimental run by using post-selection.

6.2 Post-selection

The probability of detecting no events (per an experimental run), or "vacuum" is given by:

$$P_{n=0} = e^{-\lambda}. \tag{24}$$

I will discard such events and find the distribution of "real" clicks, i.e. for $n = 1, 2, 3, ...$ Discarding the "vacuum" events requires re-normalisation of the detection distribution yielding to:

$$P_n = e^{-\lambda}\frac{(\lambda)^n}{n!} \cdot \frac{1}{c}, \quad n = 1, 2, 3, ... \tag{25}$$

where c is the normalization constant given by:

$$c = \Sigma_{n=0}^{\infty}\frac{\lambda^n}{n!} = 1 - e^{-\lambda}. \tag{26}$$

By taking the low-intensity limit $I(x) \to 0$ we get $\lambda \to 0$, which results in two outcomes. For $n = 1$ we have:

$$\lim_{\lambda \longrightarrow 0} P_{n=1} = \frac{\lambda}{e^{-\lambda} - 1} = 1 \tag{27}$$

and for $n > 1$:

$$\lim_{\lambda \longrightarrow 0} P_{n>1} = \frac{\lambda^n}{n!} \cdot \frac{1}{e^{-\lambda} - 1} = 0 \tag{28}$$

Hence, the post-selection of only non-vacuum detection events (real clicks) yields the corresponding distribution:

$$P_n = \delta_{n,1}, \quad n = 1, 2, 3, ... \tag{29}$$

Thereby, after post-selecting and taking the low intensity limit $I(x) \to 0$, the amount of detection events must either be one or none at all. This regime of parameters recreates the statistics of the particle-wave duality.

7 Conclusion and Outlook

I was able to reproduce a real-time simulation of the quantum particle interference observed in the quantum double-slit experiment using a classical electromagnetic wave. This framework relies heavily on the statistical Poisson model derived in section 6. The proof of the Poisson limit theorem for this statistical model demonstrates a theoretical basis for the existence of a regime in classical wave mechanics in which it is possible to observe particle-like interference of classical waves, or a so-called "classical wave-particle duality". To my knowledge a simple real-time simulation of this phenomena has not been established prior to this work.

Despite demonstrating a successful simulation of particle interference with waves - "classical wave-particle duality", this model will fail to reproduce other quantum phenomena such as the Hong-Ou-Mandel Effect [21] or quantum entanglement [22]. To a significant degree the flaw of my model lies in the Poissonian characteristics of the attenuated classical wave. Although the simulation snapshots in section 5 clearly indicate a single detection event for one experimental run, I believe that the if the α parameter was used to evaluate this model the outcome would indicate a value of $\alpha \simeq 1$ [12].

This demonstration of the "classical wave-particle duality" uses a clear mathematical framework as well as providing a practical demonstration thereof, enabling the model to go beyond the format of a *Gedankenexperiment*. Although, a conceptually novel idea in deriving a classical interpretation of quantum particle interference or the particle-wave duality is not established [14][23][24]. This work contributes to solidifying the distinction between quantum and classical theory whilst providing a recent summary on the relevance of classical wave mechanics and statistical models in evaluating interference experiments.

8 Appendix

Simulation code for the double-slit interference of a classical electromagnetic wave.

```
import numpy as np
import math as math
import matplotlib.animation as animation
from matplotlib import colors
import matplotlib.pyplot as plt

from mpl_toolkits import mplot3d
from matplotlib import cm
from matplotlib.ticker import LinearLocator, FormatStrFormatter



mu = 0.6
"""efficiency of detector"""
N = 1000
"""detector number- corresponds to screen length in detectors"""
M = 1000
""" detector screen width in point detectors"""
L = 10**(-6)
"""length of slit"""
d = 2
""" distance to detector screen in meters"""
a = pow(10,-9)
"""source width in point detectors"""
T = 1000
"""running time"""
r = np.zeros((N,M))
"""placeholder probability of clicks matrix"""
k = 2*np.pi*pow(10,9)
i = complex(0,1)
def p1(I):
    return I0*I
"""probability of the n-th detector clicking"""
def p0(I):
    return 1-p1(I)
"""probability of the n-th detector not clicking"""
dummy = np.zeros((N,M))
fig = plt.figure()
ims =[]
```

```
"""Define Colour Map """
cmap = colors.ListedColormap(['white', 'black'])
bounds=[0,1,10000000]
norm = colors.BoundaryNorm(bounds, cmap.N)


for t in np.arange(T):
    dummy = np.add(dummy,r)
    im = plt.imshow(dummy, animated=True, cmap=cmap, norm=norm)
    ims.append([im])
    #print(dummy)
    #print(r)
    for x in np.arange(M):
       I = math.cos(x*k*L/(d*2))**2
       #print(I)
       I0 = 1/(N*M)

       for y in np.arange(N):
          r[y,x]= np.random.choice(2,p=[p0(I),p1(I)])

"""animated plot"""
ani = animation.ArtistAnimation(fig, ims, interval=50, blit=True, repeat=False)


plt.ylabel("clicks on y axis")
plt.xlabel("clicks on x axis")
plt.title("Detection of a Classical Wave on the Detection Screen")
plt.show()


"""tosaveimageUncommentbelow"""
writergif = animation.PillowWriter(fps=30)
ani.save("dualityplot.gif",writer=writergif)
```

References

[1] Schilpp P. A. *Albert Einstein: Philosopher, Scientist*, volume VII. MJF Books: New York, 1951.

[2] P. Billingsley. *Probability and Measure*. John Wiley and Sons, Inc., 3 edition, 1995.

[3] V.B. Berestetskii, E.M. Lifshitz, and L.P. Pitaevskii. *Quantum Electrodynamics: Volume 4*. Course of theoretical physics. Elsevier Science, 1982.

[4] A. DOUGLAS STONE. *Einstein and the Quantum: The Quest of the Valiant Swabian*. Princeton University Press, 2013.

[5] A. Plotnitsky. *Niels Bohr and Complementarity: An Introduction*. SpringerBriefs in Physics. Springer New York, 2012.

[6] G. Grynberg, A. Aspect, C. Fabre, and C. Cohen-Tannoudji. *Introduction to Quantum Optics: From the Semi-classical Approach to Quantized Light*. Cambridge University Press, 2010.

[7] Leighton R. B. Feynman R. P. and Sands M. *The Feynman Lectures on Physics: Definitive Edition.* Pearson AddisonWesley, 2005.

[8] R.P. Feynman, R.B. Leighton, and M. Sands. *The Feynman Lectures on Physics, Vol. III: The New Millennium Edition: Quantum Mechanics*. The Feynman Lectures on Physics. Basic Books, 2011.

[9] A. Pais. Einstein and the quantum theory. *Rev. Mod. Phys.*, 51:863–914, Oct 1979.

[10] Philippe Grangier. *Experiments with Single Photons*, pages 135–149. Birkhäuser Basel, Basel, 2006.

[11] Alain Aspect and Philippe Grangier. *The First Single Photon Sources and Single Photon Interference Experiments*. 02 2019.

[12] John F. Clauser. Experimental distinction between the quantum and classical field-theoretic predictions for the photoelectric effect. *Phys. Rev. D*, 9:853–860, Feb 1974.

[13] M. Ueda et al. Picosecond time-resolved photoelectric correlation measurement with a photon-counting streak camera. *Optics and Communications*, 65(5), 1988.

[14] J.R. Klauder and E.C.G. Sudarshan. *Fundamentals of Quantum Optics*. Dover books on physics. Dover Publications, 2006.

[15] A. Barut, A.C. Barut, and A. Barut. *Foundations of Radiation Theory and Quantum Electrodynamics*. Springer US, 1980.

[16] D. Meschede. *Optics, Light and Lasers: The Practical Approach to Modern Aspects of Photonics and Laser Physics*. Physics textbook. Wiley, 2007.

[17] G.R. Fowles. *Introduction to Modern Optics*. Dover Books on Physics Series. Dover Publications, 1989.

[18] C. Gerry, P. Knight, and P.L. Knight. *Introductory Quantum Optics*. Cambridge University Press, 2005.

[19] L. Hörmander. *The Analysis of Linear Partial Differential Operators I: Distribution Theory and Fourier Analysis*. Classics in Mathematics. Springer Berlin Heidelberg, 2015.

[20] Lucien Le Cam. An approximation theorem for the Poisson binomial distribution. *Pacific Journal of Mathematics*, 10(4):1181 – 1197, 1960.

[21] C. K. Hong, Z. Y. Ou, and L. Mandel. Measurement of subpicosecond time intervals between two photons by interference. *Phys. Rev. Lett.*, 59:2044–2046, Nov 1987.

[22] Anton Zeilinger. Experiment and the foundations of quantum physics. *Rev. Mod. Phys.*, 71:S288–S297, Mar 1999.

[23] FERGUSON S. BRANNEN H., ERIC I. The question of correlation between photons in coherent light rays. *Nature*, 178:481–482, 1956.

[24] Y Aharonov, D Falkoff, E Lerner, and H Pendleton. A quantum characterization of classical radiation. *Annals of Physics*, 39(3):498–512, 1966.